ESC
European Society
of Cardiology

Impairment of mitophagy and autophagy accompanies calcific aortic valve stenosis favouring cell death and the severity of disease

Giampaolo Morciano[1,2][†], Simone Patergnani[1,2][†], Gaia Pedriali[1], Paolo Cimaglia [1], Elisa Mikus[1], Simone Calvi [1], Alberto Albertini [1], Carlotta Giorgi[2], Gianluca Campo [1,3], Roberto Ferrari [1,3], and Paolo Pinton[1,2]*

[1]Maria Cecilia Hospital, GVM Care&Research, 48033 Cotignola, Italy; [2]Department of Medical Sciences, Section of Experimental Medicine, Laboratory for Technologies of Advanced Therapies (LTTA), University of Ferrara, Via Fossato di Mortara, 70, 44121 Ferrara, Italy; and [3]Cardiovascular Institute, Azienda Ospedaliero-Universitaria Sant'Anna, 44121 Ferrara, Italy

Time for primary review: 31 days.

Aims	In the last 15 years, some observations tried to shed light on the dysregulation of the cellular self-digestion process in calcific aortic valve stenosis (CAVS), but the results obtained remain still controversial. This work is aimed to definitively establish the trend of autophagy in patients affected by CAVS, to analyse the putative involvement of other determinants, which impact on the mitochondrial quality control mechanisms and to explore possible avenues for pharmacological interventions in the treatment of CAVS.
Methods and results	This observational study, performed exclusively in *ex vivo* human samples (cells and serum), by using biochemical approaches and correlations with clinical data, describes new biological features of the calcified valve in terms of mitochondrial dysfunctions. In detail, we unveiled a significant deficiency in mitochondrial respiration and in ATP production coupled to increase production of lactates. In addition, mitochondrial population in the pathologic group is aged with significant alterations in biogenesis and mitophagy pathways. We are also reporting an updated view about autophagy accompanying the calcification process and advanced stages of the disease. We provided evidence for a rapamycin-based therapeutic strategy to revert the calcified phenotype to the wild type one.
Conclusion	Our data suggest that the CAVS phenotype is featured by defects in mitochondrial quality control mechanisms and that autophagy is not activated enough to counteract cell death and sustain cell functions. Thus, boosting autophagy and mitophagy from short- to long-term reverts quite all pathological phenotypes.

*Corresponding author. Tel: +39 0532 455802; fax: +39 0532 455351, E-mail: paolo.pinton@unife.it
†The first two authors contributed equally to the study.

Graphical Abstract
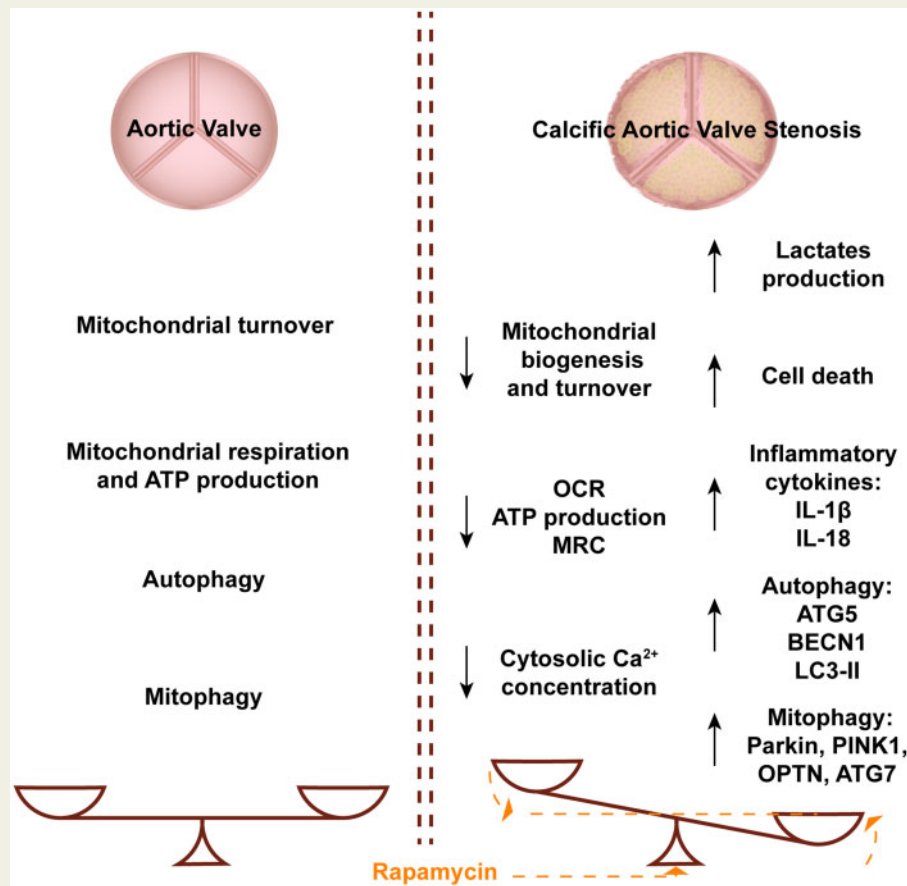
1. Introduction

Calcific aortic valve stenosis (CAVS) is the most common valvular disease of the heart and, yet, its pathogenesis is poorly understood.[1] The calcification process includes the synergistic contribution of inflammation,[2] lipid deposition,[3] oxidative stress,[4] mitochondrial dysfunctions,[5] and a genetic reprogramming in favour of the expression of osteogenic-like genes, comparable to those involved in skeletal bone development.[6] Calcification is responsible for a limited leaflet motility overtime and a progressive thinning of the area remaining functional; this involves pressure overload, hypertrophy, cardiac dysfunction, and heart failure.[5] Symptoms only occur when the valve becomes severely calcified and no pharmacological treatments are available to solve or to slow down the development of advanced CAVS. Thus, surgical aortic valve (AV) replacement becomes necessary. Despite the standards in cardiovascular surgery have improved (e.g. by transcatheter procedures and replacement valves made by either autologous or bovine tissues), calcification is a recurring pathway and the establishment of new therapies is an ambitious goal.

Autophagy is a physiological process needed for cell survival and for maintaining cellular functions.[7] It is known to be dysregulated in several pathological conditions and ageing. Among those, cardiovascular stress

trigger autophagy, especially after episodes of ischaemia/reperfusion,[8] during adaptive stages of heart failure (hypertrophy)[9] and following extracorporeal circulation procedures.[10] To date, a general consensus ascribes to autophagy (and its selective forms, such as mitophagy) beneficial effects when activated early during acute insults,[11] allowing the heart to maintain bioenergetics, to remove dysfunctional organelles and thus to protect itself.[12] Nevertheless, autophagy may also exert detrimental effect. Indeed, it has been reported that a continuous removal of mitochondria, accompanied by an imbalance in biogenesis and in other mitochondrial quality control mechanisms lead to further damage.[12]

In the last 15 years, since the first description of autophagy,[13] surprisingly, only two major studies have investigated the role of autophagy in CAVS.

The first one, in 2017 by Deng et al.,[14] reported significant higher autophagy in healthy valves compared to calcific ones ascribing to this pathway the ability to counteract pro-osteogenic reprogramming characterizing CAVS phenotype. On the contrary, in 2019, higher levels of autophagy have been found by Carracedo et al.[15] in calcified valves allowing cells to survive and be protected from the degradation process. These discrepancies in the preliminary setting about autophagy levels, and its role,[11] prompted us to investigate this issue further.

Our line of research was aimed to (i) definitively establish the trend of autophagy mainly in human aortic valve interstitial cells (HAVICs) of patients with CAVS and subjected to cardiac surgery, but also in serum samples of the same cohorts; (ii) analyse the putative involvement of the mitochondria-selective removal process, named as mitophagy, which has never being investigated before, and (iii) explore possible avenues for pharmacological interventions in the treatment of CAVS.

2. Methods

2.1 Patients

A total of 104 between patients and age-matched volunteers participated in the study.

AV cusps were obtained from 59 patients undergoing surgical aortic valve replacement (SAVR) at Maria Cecilia Hospital, Cotignola (RA), Italy, from March 2018 to July 2019. Inclusion criteria were (i) age >18 years, (ii) clinical indication to SAVR, and either (iii) severe degenerative CAVS group (44 patients), or (iv) AV without significant calcification as detected by previous echocardiogram and visual observation; in this latter group, the indication to SAVR was aortic root aneurysm (ARA group) (15 patients). ARA leads to functional aortic regurgitation due to outward displacement of AV commissures, restrictive movement of the cusps and, finally, coaptation defect. Importantly, this can happen in presence of normal non-calcific cusps. Therefore, given the impossibility in retrieve healthy post-mortem valves due to the approved Ethical Committee, these patients represent the control group. Patients with end-stage renal disease, bicuspid AV, rheumatic AV disease, non-severe aortic stenosis, mild or moderate calcification of AV cusps or infective endocarditis were excluded, as well as those not willing to participate or not able to give informed consent.

The remaining were healthy age-matched volunteers ($n = 45$) belonging to a large-scale enrolment for one of our previous studies[16] and approved by the local committee for medical ethics in research. Briefly, they are 20 women with a mean of 75 ± 8 years old and 25 men with 77 ± 7 years old. All patients gave informed consent before the inclusion and the study was carried out in accordance with the Declaration of Helsinki and following approval from the ethics committee (project no 590/2017).

2.2 Blood sample collection

Blood samples from every participant were collected in serum separator tubes and centrifuged within 2 h at $1700\,g$ at $4°C$ for 15 min. The serum obtained was stored in aliquots, coded, frozen, and stored at -80°C until assay.

2.3 HAVIC isolation

HAVICs, immediately after the AV removal by the surgeon, were isolated following a modification of a previously described method.[17] Valve leaflets were rinsed in phosphate buffered saline (PBS) and then digested in collagenase II (Sigma-Aldrich, C6885, 2.5 mg/mL in Medium 199, Earle's Salts, Sigma-Aldrich, M2154) for 15 min at 37°C. After removing endothelial cells by scraping, the leaflets were broken into small pieces and further digested with a milder solution of collagenase medium (0.8 mg/mL) for 3 h at 37°C. After vortexing and aspirating repeatedly to break up the tissue mass, the cell suspension was spun at $100\,g$ for 10 min to remove any remaining tissue. The supernatant was filtered through a $100\,\mu M$ cell strainer (Falcon® Cell Strainers, 352360) and transferred into a fresh tube and spun again at 1200 rpm for 5 min at

4°C. The cells were resuspended in full medium [M199 containing 2 mM L-glutamine, 10% foetal bovine serum, and $1\times$ Penicillin-streptomycin solution], plated onto a 75 cm^2 flask, and maintained at 37°C and 90% relative humidity in 5% CO_2. When the cells reached 70–90% confluence, they were subcultured on plates and chamber slides.

About treatment with rapamycin, a concentration of 100 nM has been used for 3 h and 7 days (only where long-term treatment is indicated). Bafilomycin A1 (BAF-A1) has been used 10 nM for 3 h.

2.4 Transfection

HAVICs were transfected with HiPerFect Transfection Reagent (Qiagen, 301704) according to the manufacturer's instructions.

2.5 Circulating protein quantification

Serum aliquots were thawed to measure inflammation levels through the quantification of IL-1β release with an ELISA (Enzyme Linked Immunosorbent Assay) (R&D Systems, DLB50) and IL-18 with a Sandwich High Sensitivity ELISA kit (BOSTER, EK0864). It has been quantified also autophagy levels from Autophagy related 5 (ATG-5) and BECN-1 detection using two commercially available ELISA kits (My Biosource, San Diego, California, USA; codes MS7209535 and MBS732891, respectively) following the instructions of the manufacturer. For mitophagy assessment Human PTEN-induced putative kinase 1 (PINK1) and Parkin were detected in the same samples (Mybiosource, MBS9327222 and MBS732278, respectively) following the instructions of the manufacturer. It has been quantified also levels from Autophagy Related Protein 7 (ATG-7) and Optineurin (OPTN) using two commercially available ELISA kits (My Biosource, San Diego, California, USA; codes MBS062423 and MBS069530, respectively) following the instructions of the manufacturer.

Serum levels of lactate were determined using a colorimetric L-Lactate Assay Kit according to the manufacturer's protocol (L-Lactate Assay Kit Colorimetric, Abcam, ab65331).

2.6 Alizarin red

HAVICs were cultured in 35 mm cell imaging dishes (Eppendorf Cell Imaging Dish, 0030740017) 24 h before the experiments. Then, cells were washed with PBS and fixed in 4% paraformaldehyde for 15 min at room temperature, then stained with 2% solution of alizarin red (pH 4.2) for 15 min washed three times with PBS. Images were taken with Nikon upright Microscope Ni equipped with digital High-definition Color Camera Head DS-Fi2 5-megapixel CCD and $20\times$ air lens. Successively, the stain was solubilized in 10% (v/v) acetic acid by shaking for 30 min. The absorbance of the released Alizarin red stain was measured using microplate reader at a wavelength of 405 nm.

2.7 Immunoblot

For immunoblotting, cells were lysed in radioimmunoprecipitation assay buffer, then quantified by the Lowry method and 10 μg of proteins were loaded on a 4–20% precast gel. After electrophoretic separation, proteins were transferred onto nitrocellulose membranes that were incubated overnight with primary antibodies as p62 (1:1000), glyceraldehyde-3-phosphate dehydrogenase (GAPDH) (1:5000), microtubule-associated protein light chain 3 (LC3) (1:1000), Beclin1 (BECN1) (1:1000), cleaved poly (ADP-ribose) polymerase (PARP) (1:1000), TUBB (1:5000), cleaved receptor-interacting serine/threonine-protein (RIP) (1:1000), cleaved caspase 3 (CAS3) (1:1000), dynamin-related protein 1 (Drp1) (1:1000), pDrp1 (1:1000), serine/threonine-protein kinase ULK1

(ULK1) (1:1000), pULK1 (1:1000), Ras-related protein (Rab9) (1:1000), mammalian target of rapamycin (pMTOR) (1:1000), MTOR (1:1000), pP70S6K (1:1000), P70S6K (1:1000), actin (1:5000), peroxisome proliferator-activated receptor-gamma coactivator 1-alpha (PGC1α) (1:1000), and osteocalcin (1:1000). The revelation was assessed by specific HRP-labelled secondary antibodies, followed by detection by chemiluminescence using ChemiDoc™ Touch Gel Imaging System. Western blots shown in figures are representative of at least three different independent experiments.

2.8 Detection of cell death

For annexin V staining, cells were plated onto 35 mm-well plates. After 48 h cells were gently harvested, processed with buffers, and incubated with annexin V-Cy3 solution and propidium iodide (PI) according to manufacturer's protocols (Biovision, Milpitas, CA, USA). The green and red fluorescence signals were quantified under all conditions on a Tali image-based cytometer (Invitrogen).

2.9 Oxygen consumption rate (OCR)

The rate of oxygen consumption was assayed with the XF96 Extracellular Flux Analyzer (Seahorse Biosciences—Agilent Technologies, Santa Clara, CA USA). Cells were plated 2 days before the experiment and wait until confluent monolayer. Briefly, mitochondrial respiration was evaluated measuring oxygen consumption rate (OCR) in basal conditions and after the addition of oligomycin (1 μM), carbonyl cyanide-4-(trifluoromethoxy)phenylhydrazone (2 μM), rotenone (1 μM), and antimycin A (1 μM). OCR values were normalized on cell density using the colorimetric sulforodhamine B assay.

2.10 Fluorescence microscopy

2.10.1 Autophagy detection through quantitative analysis of GFP-LC3 dots

HAVICs were cultured in 24 mm glass coverslips and transfected at 50% confluence with 2 μg of green fluorescent protein-microtubule-associated protein light chain 3 (GFP-LC3) plasmid DNA and with H2B-RFP construct to stain nuclei. After 36 h, images were taken on a Zeiss LSM510 confocal microscope equipped of a HAL 100 camera (Zeiss, Oberkochen, Germany) and a 63× oil immersion objective (N.A. 1.4). For each condition, the number of GFP-LC3 dots was counted in at least 25 independent visual fields.

2.10.2 Mitophagy detection

The microscopic analysis of mitophagy levels was evaluated essentially as described in References.[18] Briefly, HAVICs were cultured on 24 mm glass coverslips in complete medium and transfected with H2B-RFP construct to stain nuclei. Before experiments, cells were loaded with LysoTracker Red DND-99 (Life Technologies) to mark lysosomal structures (red) for 15 min. After three washes, cells were next loaded with MitoTracker Green FM (Life Technologies) to visualize mitochondria (green) for 15 min. The degree of co-localization of mitochondria with lysosomes was measured via cell live imaging microscopy at 37°C and 5% CO_2 atmosphere using a Zeiss LSM510 confocal microscope equipped of a HAL 100 camera (Zeiss, Oberkochen, Germany) and a 63× oil immersion objective (N.A. 1.4). Confocal images of single planes were acquired and analysed with identical settings. Statistical evaluation of co-localization was carried out using the co-localization counter JACOP available with Fiji software.

2.10.3 Cytosolic Ca^{2+} measurements

Basal cytosolic calcium (Ca^{2+}) and its response upon agonist administration was evaluated essentially as described in References,[19] making use of the fluorescent Ca^{2+} indicator Fura-2 AM (Life Technologies, Invitrogen). Briefly, cells were grown on 24 mm coverslips and incubated at 37°C for 30 min in 1 mM Ca^{2+}/Krebs–Ringer buffer supplemented with 2.5 μM Fura-2/AM, 0.02% Pluronic F-68 (Sigma), and 0.1 mM sulfinpyrazone (Sigma). To determine basal cytosolic Ca^{2+} ratio cells were placed in an open Leyden chamber on a 37°C thermostated stage and exposed to 340/380 nm wavelength light in resting conditions; to evaluate its response to agonists, His and BK were added to the 1 mM Ca^{2+}/Krebs–Ringer buffer, and Ca^{2+} ratio increase in the cytosol was recorded as indicated in the figures. The fluorescence data collected were expressed as emission ratios at 340/380 nm.

2.10.4 MITO TIMER measurements

Cells were transfected with the pTRE-tight-MITO TIMER plasmid. Following References,[20] cells were imaged using excitation at 490 nm and 550 nm and emission of green (500–540 nm) and red (580–640 nm) fluorescence signals by using a Zeiss LSM510 confocal microscope equipped of a HAL 100 camera (Zeiss, Oberkochen, Germany) and a 63× oil immersion objective (N.A. 1.4). The ratio of the fluorescence signal intensity in the red and green channels was determined at various time points showing progressive maturation of MITO TIMER (red conversion). Ratiometric images were generated using NIH ImageJ software.

2.11 Statistics analyses

Statistical methods included t-test (two groups), one-way ANOVA with multiple comparisons (three or more groups), and Spearman's correlation coefficient performed by GraphPad Prism 8.2 (Prism, La Jolla, CA, USA). A P-value <0.05 was considered significant. P-values are reported in the figure legends.

3. Results

3.1 Calcified valves have increased autophagy but persistent cell death

To fulfil the first aim of our research, autophagy was directly measured in the calcific AV. Due to the high calcification grade of some leaflets, not all AVs from the 44 patients with CAVS produced viable cells, the yield was about the 50% of the total. All patients gave informed consent before the inclusion and the study was carried out in accordance with the Declaration of Helsinki.

Immunofluorescences performed on HAVICs confirmed higher expression of Vimentin cell marker, as well as other proteins involved in the calcification process, such as RUNX2 and Osteocalcin in CAVS compared to ARA valves, these later are considered as non-calcific controls (Supplementary material online, Figure S1). In addition, the Alizarin red assay, an indicator of Ca^{2+} containing osteocytes, confirmed the phenotype of severely calcified valves in CAVS, as it resulted two-fold higher than ARA group (Figure 1A).

Autophagy was then assessed through immunofluorescence, upon transfection of HAVICs with GFP-LC3 construct, and by western blot by detection of specific autophagic markers, such as p62, LC3-II, and BECN1.

The number of GFP-LC3 dots counted for each cell (Figure 1B), the increases in BECN1 and LC3-II expression together with the reduced
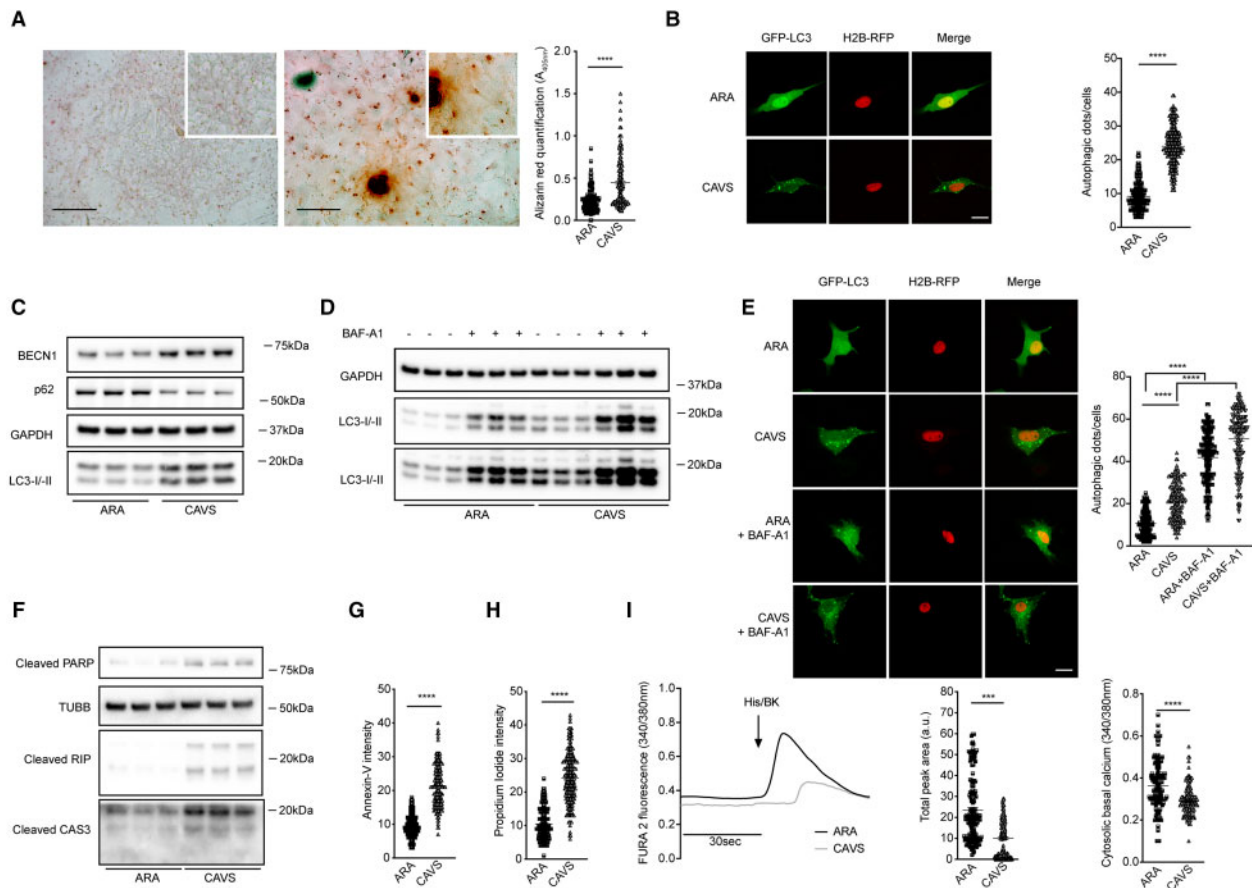
Figure 1 Evaluation of autophagy in HAVICs from CAVS and ARA patients. (A) Alizarin red assay on HAVICs from 15 ARA and 22 CAVS patients, representative images and quantification of extraction. Scale bars: 100 µm. Each value is the mean of 10 observations (2 technical and 5 biological replicates). (B) Immunofluorescence on HAVICs from 15 ARA and 22 CAVS patients showing GFP-LC3 expression and quantification of autophagic dots/cells; (red) nuclei by H2B-RFP expression; (green) GFP-LC3 dots. Scale bar: 5 µm. Each value is the mean of 20 cells (4 technical and 5 biological replicates). (C) Immunoblot detection of autophagy in HAVICs lysates. GAPDH was used as a loading marker; BECN1, p62 and LC3 as autophagic markers. This is representative of three biological replicates. (D) Immunoblot detection of autophagic flux in HAVICs lysates using BAF-A1. GAPDH was used as a loading marker; LC3 as autophagic marker. For this last one, a short exposure (top) and a long exposure (bottom) have been provided. This is representative of three biological replicates. (E) Immunofluorescence on HAVICs from 10 representative ARA and 10 representative CAVS patients showing GFP-LC3 expression treated with BAF-A1 and quantification of autophagic dots/cells; (red) nuclei by H2B-RFP expression; (green) GFP-LC3 dots. Scale bar: 5 µm. Each value is the mean of 20 cells (4 technical and 5 biological replicates). (F) Immunoblot detection of cell death in HAVICs lysates. TUBB was used as loading marker; cleaved PARP, RIP, and CAS3 as apoptotic and necrotic markers. This is representative of three biological replicates. (G) Quantification of Annexin V fluorescent signal as apoptotic marker on HAVICs from 15 ARA and 22 CAVS patients. Each value is the mean of 10 observations (2 technical and 5 biological replicates). (H) Quantification of PI fluorescent signal as necrotic marker on HAVICs from 15 ARA and 22 CAVS patients. Each value is the mean of 10 observations (2 technical and 5 biological replicates). (I) Cytosolic basal Ca^{2+} concentration and cytosolic Ca^{2+} response upon agonist-induced in living cells, quantified using FURA-2AM on HAVICs from 15 ARA and 22 CAVS patients. Each value is the mean of 20 cells (4 technical and 5 biological replicates). ARA, aortic root aneurysm; CAVS, calcific aortic valve stenosis; BAF-A1, bafilomycin A1; His/BK: histamine/bradykinin. *P*-values have been obtained by performing *t*-test for two groups and one-way ANOVA for more than two groups. *P-value <0.05; **P-value <0.01; ***P-value <0.001.

expression of p62 levels (*Figure 1C*) detected in CAVS samples altogether confirmed that autophagy is up-regulated in calcified AV compared to not calcified regurgitant AVs.

To discriminate whether the increases in the autophagic process was due to an effective activation of the autophagic flux or to an inhibition of the autophagosome–lysosome fusion, we treated the cells with BAF-A1, an inhibitor of lysosomal acidification widely used to mimic a block of the autophagic flux (*Figure 1D*). The expression of LC3-II upon BAF-A1 exposure was increased in both ARA and in CAVS cells and these data

have been confirmed also by immunofluorescence analysis (*Figure 1E*). This finding confirms that CAVS valves have more sustained autophagic levels than ARA samples, and demonstrates that this feature was not due to alteration in the autophagic flux (*Figure 1D and E*).

Figure 1F–H relates to cell death in CAVS compared to ARA group. There was a significant increase of cell death in CAVS group as measured by both higher amounts of cleaved proteins, such as PARP, RIP, and CAS3 and by increased fluorescent signal of Annexin V and PI probes (*Figure 1F–H*).
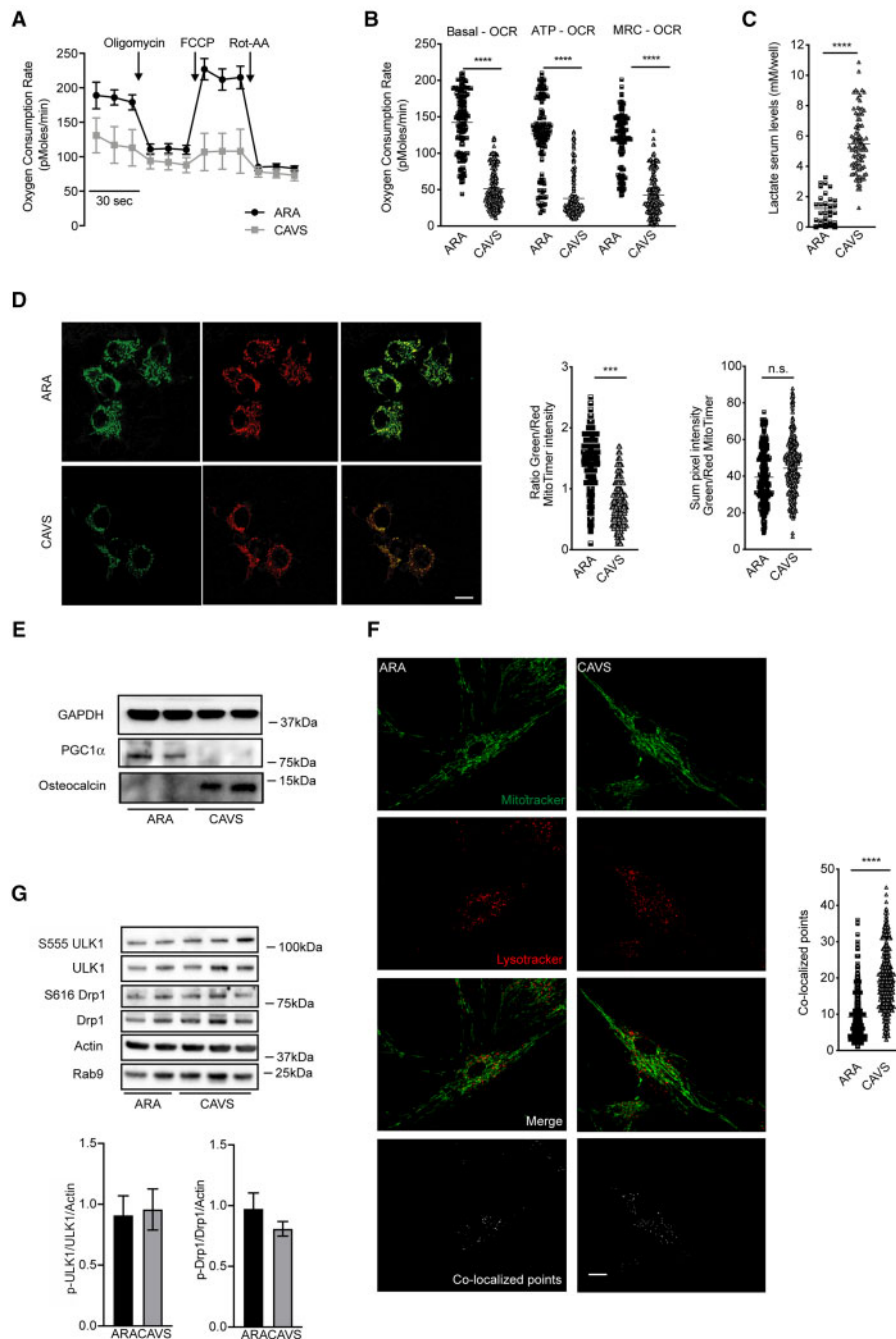
Figure 2 Mitophagy detection in HAVICs. (*A*) Respiration parameters measured in living HAVICs by Seahorse XF analyzer. (*B*) Details on the OCR quantification in HAVICs. Each value of (*A*) that is summarized in (*B*) is the mean of 9 observations (3 technical and 3 biological replicates). (*C*) Quantification of lactate levels in serum samples from 15 ARA and 44 CAVS patients. Each value is the mean of the absorbance of two wells from the Elisa Kit used. (*D*) MITO TIMER measurements of mitochondrial age of HAVICs from 15 ARA and 22 CAVS patients. Representative images of the green, the red channels, and the merge are shown with statistics. Scale bar: 5 μm. Each value is the mean of 20 cells (4 technical and 5 biological replicates). (*E*) Immunoblot showing mitochondrial biogenesis in HAVICs lysates. GAPDH was used as loading marker; PGC1α as mitochondrial biogenesis marker and Osteocalcin as calcification marker. This is representative of three biological replicates. (*F*) Co-localization analysis between LysoTracker Red DND-99 to mark lysosomal structures (red) and MitoTracker Green FM to visualize mitochondria (green) as index of mitophagic process from 15 ARA and 22 CAVS patients. Scale bar: 5 μm. Each value is the mean of 20 cells (4 technical and 5 biological replicates). (*G*) Immunoblot showing phosphorylations of Ser616 of Drp1, Ser555 of ULK1, Drp1, ULK1, and Rab9. Actin was used as loading marker. This is representative of three biological replicates. *P*-values have been obtained by performing one-way ANOVA test for multiple comparisons and *t*-test for comparisons between two groups. *P-value <0.05; **P-value <0.01; ***P-value <0.001.

Downstream analysis in living cells also shows the presence of a dysregulated Ca^{2+} dynamics. Cytosolic Ca^{2+} in CAVS cells was reduced compared to ARA group, both in terms of basal Ca^{2+} and of the response to agonist administration (*Figure 1I*).

3.2 Mitochondrial function and mitophagy in CAVS

Studies in different pathological conditions have demonstrated that intracellular Ca^{2+} fluxes and autophagy are determinant for the correct maintenance of cellular bioenergetic.[21] In particular, both degree of autophagy and Ca^{2+} can activate and modulate the mitochondrial oxidative phosphorylation and ATP production.[22] In view of the altered levels of Ca^{2+} dynamics and the increased autophagy in CAVS, we decided to determine the state of the mitochondrial respiration in these cells. By using Seahorse XF analyzer, we recorded in CAVS a significant decrease in mitochondrial OCR (*Figure 2A*), a lack of ATP production and a lower maximal respiration capacity compared to ARA, suggesting mitochondria uncoupling (*Figure 2B*). These changes were concomitant with an increased lactate production (*Figure 2C*), probably in the effort to produce anaerobic ATP through glycolytic activity.

Data reported in *Figure 2* refer to processes aimed to control mitochondrial quality and function of HAVICs. To preserve a functional and healthy mitochondrial population, the cells must replace defective mitochondria with others newer and more functional. Such mitochondrial turnover is guarantee by several mechanisms; the most important is the ratio between mitophagy and the mitochondrial biogenesis. To explore mitochondrial turnover, we used the fluorescent plasmid MITO TIMER, which labels in green newly synthetized mitochondria, while the fluorescence shift to red when the mitochondrial population is aged. The fluorescence obtained indicates that CAVS mitochondria are significantly older and less functional than those of the ARA valve (*Figure 2D*). Mitochondrial biogenesis was also assessed by measuring the expression of PGC1α, which, in turn, was strong down-regulated in CAVS (*Figure 2E*). Taken together, an increased cell death accompanied by reduced biogenesis and aged mitochondrial population, suggests a defect in mitochondrial turnover.

We then investigated mitophagy on isolated HAVICs and our data suggested a significant increase in mitophagy as measured by the co-localization analysis between lysotracker (marker for lysosomes) and mitotracker (marker for mitochondria) fluorescent probes (*Figure 2F*).

Recently, Saito *et al.*[23] showed how mitophagy can be activated *in vivo* upon energy stress, such as ischaemia, through an alternative pathway, which does not include Parkin and PINK1 but involves the ULK1/Rab9/RIP1/Drp1 axis. Indeed, the formation of that multiprotein complex, triggered by a phosphorylation cascade (S555 of ULK1, S179 of Rab9, and S616 of Drp1) allow for Drp1-dependent mitochondrial fragmentation and mitophagy. Although we are not in the presence of an ischaemic episode, but given the fact that mitophagy can undergo alternative pathways *in vivo*,[23] we investigated whether mitophagy observed in CAVS might follow the ULK1/Rab9/RIP1/Drp1-dependent pathway. To this aim, we analysed the phosphorylation status of both ULK1 at S555 and Drp1 at S616 without significant differences between ARA and CAVS samples (*Figure 2G*).

3.3 Autophagy and mitophagy are up-regulated in serum of CAVS patients and correlates with advanced cardiac disease

To further evaluate autophagy in CAVS, the autophagic biomarkers ATG5 and BECN1 have been detected and quantified in sera from the

same cohort of patients in *Figures 1 and 2*: 44 patients with AS, 15 patients with ARA (*Table 1* and Section 2), and 45 additional healthy volunteers. All patients gave informed consent before the inclusion and the study was carried out in accordance with the Declaration of Helsinki. There were increasing ATG5 values from healthy volunteers (10.17 ± 0.37 ng/mL for ATG5) to ARA group (13.54 ± 0.62 ng/mL for ATG5) and to CAVS (18.80 ± 0.67 ng/mL for ATG5), but not for BECN1 levels, which differences become significant only between ARA and CAVS or healthy volunteers and CAVS. Overall, circulating autophagic proteins in CAVS were significantly higher than in control population as well in patients with ARA (*Figure 3A and B*). Inflammatory cytokines levels were also significantly higher in CAVS (99.28 ± 10.30 pg/mL for IL-1β and $2817 \pm 307,1$ pg/mL for IL-18) compared to the two other groups (healthy volunteers: 28.66 ± 1.59 pg/mL for IL-1β and 1025 ± 190.1 pg/mL for IL-18; ARA: 17.93 ± 0.55 pg/mL for IL-1β and 1310 ± 244.9 pg/mL for IL-18) (*Figure 3G and H*). Both biomarkers of autophagy were strongly correlated with IL-1β (Spearman's $R = 0.54$ for ATG5 and 0.66 for BECN1) (Supplementary material online, *Figure S2A and C*), slightly less with IL-18 levels (only for BECN1, Supplementary material online, *Figure S2D*) and no correlation between ATG5 and the latter cytokine (Supplementary material online, *Figure S2B*).

At the same time, to confirm results obtained in *Figure 2*, mitophagy in CAVS sera has been investigated with the biomarkers Parkin, PINK1, ATG7, and OPTN, quantified from the same cohort of patients. There were higher levels of mitophagy in CAVS (482.6 ± 28.46 pg/mL for Parkin, 6.08 ± 0.36 ng/mL for PINK1, 7.16 ± 0.40 ng/mL for OPTN, and 11.84 ± 0.83 ng/mL for ATG7) compared to ARA (353.8 ± 11.61 pg/mL for Parkin, 1.49 ± 0.15 ng/mL for PINK1, 3.87 ± 0.48 ng/mL for OPTN, and 6.13 ± 0.66 ng/mL for ATG7) and healthy volunteers (271.3 ± 9.34 pg/mL for Parkin, 2.65 ± 0.16 ng/mL for PINK1, 2.83 ± 0.25 ng/mL for OPTN, and 1.01 ± 0.04 ng/mL for ATG7) (*Figure 3C–F*). These biomarkers, like those for autophagy, were highly correlated to IL-1β production (Supplementary material online, *Figure S2E, G, I and K*), to IL-18 for ATG7 and Parkin (Supplementary material online, *Figure S2F and J*) and no correlation with IL-18 for OPTN and PINK1 proteins (Supplementary material online, *Figure S2H and L*).

To explore possible links between autophagy/mitophagy and the clinical features of CAVS patients, *Table 1* reports the main characteristics of the two populations: patients with aortic stenosis and those with ARA. No significant differences were detected between groups and the percentage of comorbidities and of risk factors were similar. The same holds true for the laboratory's variables. As expected, patients with ARA showed larger end-systolic and end-diastolic volumes while those with AS showed a higher trans-valvular gradient.

Moreover, at univariable analysis, no clinical characteristic is associated with AS/ARA status; we have a slightly association only with age (Supplementary material online, *Table S1*). However, noteworthy, at multivariable analysis, autophagic and mitophagic biomarkers are independently associated with AS/AR status (Supplementary material online, *Table S1*). The healthy volunteers were age-matched with the two groups. All were free from comorbidities.

At this point, CAVS patients have been stratified according to the median value of ATG5 (17 ng/mL), BECN1 (5 ng/mL), ATG7 (8 ng/mL), and OPTN (6 ng/mL). As shown in *Figure 3I and J*, patients with ATG5, BECN1, ATG7, and OPTN levels above the median value had a greater left ventricle end-systolic volume (LV ESVi) ($P < 0.05$), an index of critical and advanced clinical condition.

Despite the CAVS population of the study was mostly homogeneous to ensure the reproducibility of data obtained to achieve our first main

Table 1 linical features of the population study

	Aortic stenosis (n = 44)	Aortic root aneurysm (n = 15)	P
Age (years)	76 [72–78]	70 [65–78]	0.139
Male sex	19 (43)	11 (73)	0.05
BMI (kg/m^2)	28 [24–30]	27 [24–29]	0.644
Medical history			
Hypertension	38 (86)	15 (100)	0.322
Dyslipidaemia	33 (75)	10 (67)	0.522
Diabetes	3 (7)	0 (0)	0.564
Smoke			0.604
Never	16 (36)	4 (22)	
Prior	21 (48)	8 (45)	
Current	7 (16)	6 (33)	
CAD	18 (41)	6 (40)	0.951
Prior stroke	1 (2)	0 (0)	0.999
PAD	7 (16)	2 (13)	0.999
AF	9 (21)	5 (33)	0.316
COPD	7 (16)	2 (13)	0.999
Laboratory data			
Haemoglobin (g/dL)	13.4 [12.7–14.3]	13.7 [12.4–14.5]	0.887
Glucose (mg/dL)	101 [93–110]	95 [90–121]	0.917
eGFR (mL/min)	68 [57–90]	57 [43–79]	0.133
Albumin (g/dL)	4.2 [4.1–4.4]	4.4 [4.1–4.7]	0.116
LDL (mg/dL)	95 [75–115]	92 [76–99]	0.746
Echocardiography data			
LV EDVi (mL/m^2)	44 [36–56]	87 [72–119]	<0.001
LV ESVi (mL/m^2)	18 [12–22]	41 [25–49]	<0.001
LV EF (%)	62 [55–68]	59 [45–65]	0.241
LVMI (g/m^2)	114 [98–138]	141 [108–191]	0.067
AV MPG (mmHg)	45 [38–53]	8 [6–21]	<0.001
AV peak velocity (m/s)	4.3 [4.0–4.6]	1.9 [1.7–2.9]	<0.001

Continuous variables are presented as median [interquartile range], categorical variables are presented as count and percentage.
Comparison between groups was performed with independent sample t-test, Mann–Whitney U test, Pearson's χ^2 test, or Fisher's exact test, as appropriate.
BMI, body mass index; CAD, coronary artery disease; PAD, peripheral artery disease; AF, atrial fibrillation; COPD, chronic obstructive pulmonary disease; CKD, chronic kidney disease; eGFR, estimated glomerular filtration rate; LV, left ventricle; EDVi/ESVi, end diastolic/systolic volume index; EF, ejection fraction; LVMI, left ventricle mass index; AV, aortic valve; MPG, mean pressure gradient.

aim, we tried to find any correlations between the calcification grade of the valve and both autophagy and mitophagy levels in that population. The calcification grade has been measured by Alizarin red staining and by the computed tomography aortic valve calcium score (CT-AVC, which was not available for all patients enrolled, because it is a clinical test used for prevention but not mandatory for those patients undergoing surgery) and matched with biomarkers measured in sera. We found a trend of positive correlation for mitophagy assuming significant values only for OPTN towards Alizarin red and OPTN/PINK1 for CT-AVC (*Figure 3K and L*).

3.4 Induction of autophagy reverts most features of the CAVS phenotype

Our data demonstrated that CAVS are characterized by increased levels of autophagy, cell death and mitophagy, with aged mitochondria not able

to be renewed. We then tested the hypothesis that further boosting autophagy improves the elimination of dead cells and ameliorate the calcified phenotype.

Rapamycin is a recognized inducer of autophagy[24] by modulating the MTOR pathway and its substrate P70S6K. *Figure 4* shows that 3 h treatment of 100 nM rapamycin suppresses phosphorylated MTOR and P70S6K (*Figure 4A*). At the same time, *Figure 4B* shows CAVS cells treated with rapamycin increased the autophagic dots as measured by GFP-LC3 fluorescence and mitophagy detected by a co-localization analysis between lysotracker and mitotracker (*Figure 4C*). This pharmacologically induced autophagy and mitophagy reduced cell death as evaluated by cleaved PARP, CAS3, and RIP markers, as well as Annexin V and PI (*Figure 4D–F*). Long-term treatments (7 days) with rapamycin ameliorated the calcified phenotype by decreasing Ca^{2+} containing osteocytes signal measured by alizarin red staining (*Figure 4G*). Rapamycin also partially restored the overall intracellular Ca^{2+} dynamics. Indeed, when CAVS samples were treated with rapamycin, we observed significant recovering of the basal intracellular Ca^{2+} levels. Despite this, rapamycin failed to improve Ca^{2+} increases following agonist stimulation (*Figure 4H*).

4. Discussion

There are few and controversial information on the role of autophagy in the pathophysiology of AS and no data are available of either mitochondrial function or mitophagy. We believe that our translational data shed some light on the role of auto- and mitophagy in CAVS. The first aim was to define the trend of autophagy mainly in the valvular tissue, but also in sera of the same patients. The use of autophagic proteins in sera to investigate about the existence of a link between autophagy dysregulation and a given disease is well-established in the literature[16,25,26] albeit the ultimate source of these circulating markers often is not known.

The increases of both GFP-LC3 dots and BECN1/LC3-II proteins expression with a parallel decrease of p62 detected in the living cells of CAVS patients, as well as the higher levels of circulating ATG5 and BECN1 in serum samples, confirm the findings of Somers et al.[13] in 2006 and Carracedo et al.[15] in 2019 that the autophagic process is elevated in CAVS. In the first report, Somers found autophagy as the main mechanism available to calcified cells to die; while the second one sees it as a survival pathway to avoid the completely loss of cell functions. Our data, that bring an important update and novelty in this field, are placed in the middle of both reports. Indeed, they show that increased autophagy in CAVS was associated to cell death, which likely is a consequence of insufficient organelle removal and subsequent protein recycle necessary for cell life. Despite our population of CAVS was mostly homogeneous to ensure reproducibility of data investigated for our main aim, interestingly, we also found that highest levels of autophagy (above the median value) were related to an advanced stage of the disease, and this constitutes an important update to the knowledge.

Furthermore, for the first time, and this is the second aim of our study that also represent a novelty in the field, we reported an increased mitophagy in the calcified valves and a series of mitochondrial impairments. Indeed, defected mitophagy was not the only alteration of mitochondria in CAVS patients. Our data show the presence of aged mitochondria with reduced respiratory capacity despite an increased auto- and mitophagic activity. This, in turn, could be the consequence of additional deficits, such as impaired mitochondrial biogenesis, insufficient mitochondrial renewal and turnover, despite the increased mitophagy.
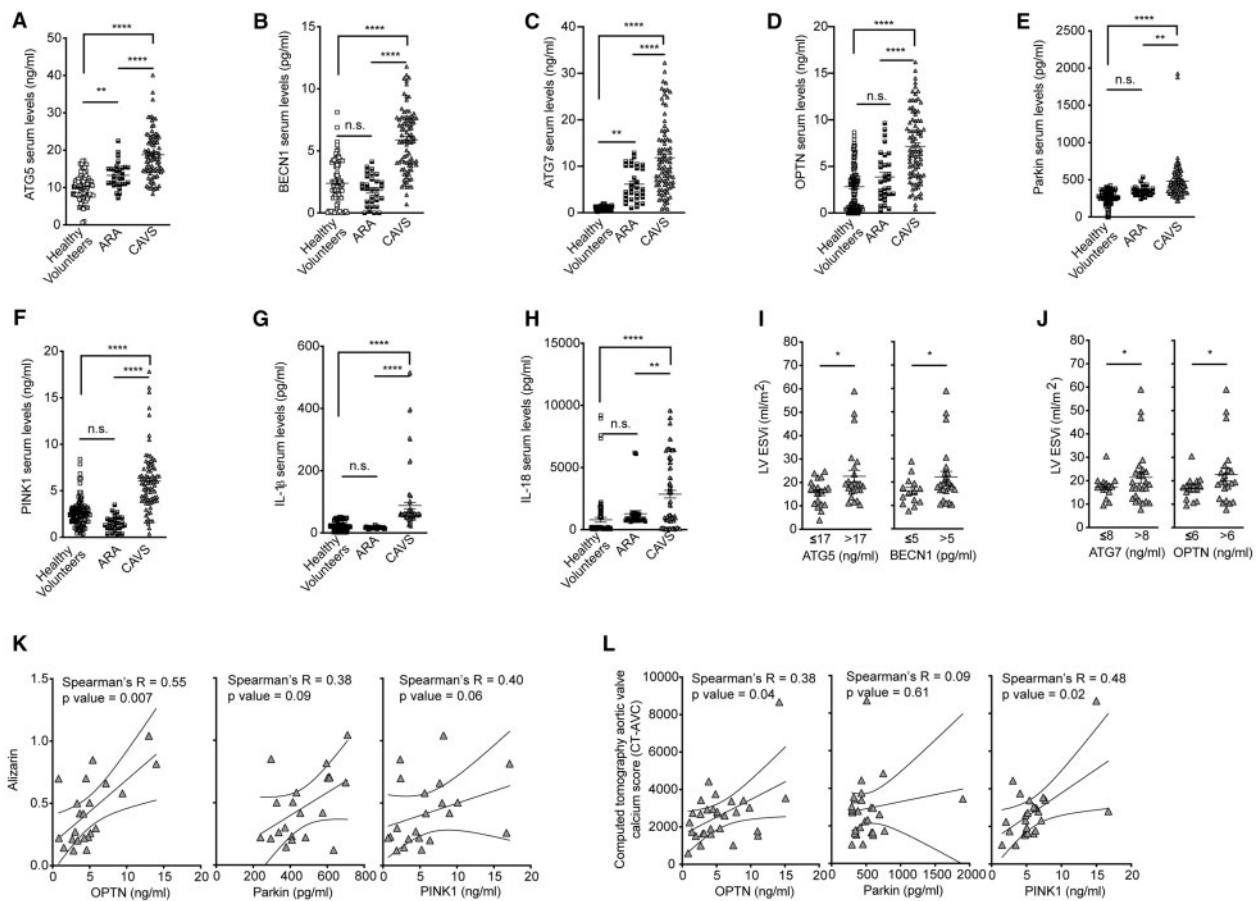
Figure 3 Autophagic and mitophagic markers and inflammatory cytokines detection in patients' sera and calcification grade. (A) Quantification of ATG5, (B) BECN1, (C) ATG7, (D) OPTN, (E) Parkin, (F) PINK1, (G) IL-1β, (H) IL-18 serum levels from 45 healthy volunteers, 15 ARA, and 44 CAVS patients. From (E) two CAVS values have been excluded as above the maximum limit of the reference scale. From (F) four CAVS values have been excluded as above the maximum limit of the reference scale. Each point reported is the mean of the absorbance from two wells of the corresponding Elisa Kit used. (I) Correlation between LV ESVi value and ATG5 and BECN1 levels in the 44 CAVS cohort only. (J) Correlation between LV ESVi value and ATG7 and OPTN levels in the 44 CAVS cohort only. (K) Correlation between quantification of extracted alizarin red on HAVICs from 22 CAVS patients and OPTN (22 points of correlation), Parkin (20 points of correlation), and PINK1 (21 points of correlation) serum levels of the same patients. (L) Correlation between CT-AVC from 29 CAVS patients and OPTN (29 points of correlation), Parkin (28 points of correlation), and PINK1 (25 points of correlation) serum levels of the same patients. P-values have been obtained by performing one-way ANOVA test for multiple comparisons, t-test for comparisons between two groups, and Spearman's correlation test for correlations. *P-value <0.05; **P-value <0.01; ***P- value <0.001.

Not only highest levels of mitophagy were significantly related to an advanced stage of the disease, but mitophagy also assumes a positive trend in line with the calcification grade of the valve, which becomes statistically significant in the case of OPTN and PINK1.

Mitophagy can be activated by either 'canonical' pathways (Parkin- and PINK1-dependent)[27] or by alternative routes (Parkin-independent).[23] Our data would exclude a Drp1-dependent pathway, depending in turn by the upstream regulator ULK1/Rab9/RIP1 axis, as no differences in the phosphorylation status of both ULK1 S555 and Drp1 S616 have been detected. Contrarily, having observed increased levels of Parkin, PINK1, and the LC3-II receptor OPTN in sera, as well as the findings about LC3-II and the adaptor p62 in HAVICs,[28] our data suggest the involvement of the *canonical* pathway.

Taken together, these results are interesting as they are amenable of therapeutic interventions aimed at increasing the cellular autophagic processes. This was the third aim of our work.

Rapamycin and several analogues are potent inducers of autophagy, they are safe and currently used in therapy. Boosting autophagy with rapamycin in CAVS cells, which already express high autophagic flux, further ameliorated the diseased phenotype, including cell death, one of the major CAVS features, which was reverted. Noteworthy, long-term treatment of rapamycin also reduced Ca^{2+} containing osteocytes detected by alizarin red. The observed beneficial effects of rapamycin are in agreement with previous studies in different pathological conditions in which the use of rapamycin significantly increases mitochondrial efficiency.[29–31] However, in our hand, Ca^{2+} dysregulation was only partially restored. Rapamycin, indeed, augmented the resting Ca^{2+} levels, but failed to improve Ca^{2+} increases following agonist stimulation. This could be due to the variability degree of calcification and to different characteristics of patients subjected to cardiac surgery. Furthermore, we cannot exclude that the properties of channels and pumps regulating the Ca^{2+} movement may be affected during the different phases, which
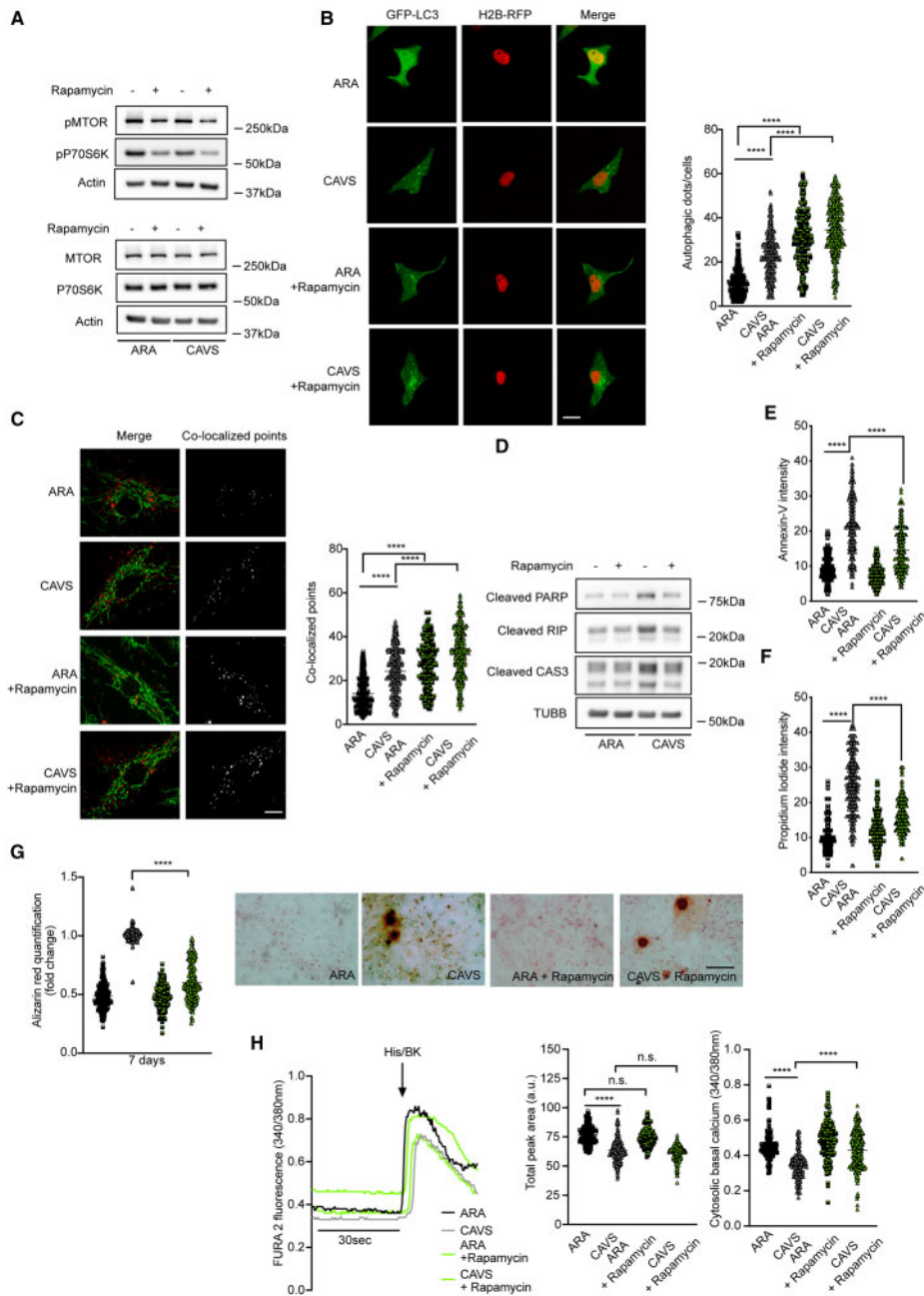
Figure 4 Modulation of autophagic and mitophagic processes in HAVICs with rapamycin. (*A*) Immunoblot of rapamycin efficacy on HAVICs cell lysates. Actin was used as loading control, pMTOR and pP70S6K decrease as readout of rapamycin treatment as widely published elsewhere. This is representative of three biological replicates. (*B*) Immunofluorescence showing GFP-LC3 expression in HAVICs from 15 ARA and 22 CAVS treated or not with rapamycin and quantification of autophagic dots/cells; (red) nuclei by H2B-RFP expression; (green) GFP-LC3 dots. Scale bar: 5 μm. Each value is the mean of 20 cells (4 technical and 5 biological replicates). (*C*) Co-localization analysis between LysoTracker Red DND-99 to mark lysosomal structures (red) and MitoTracker Green FM to visualize mitochondria (green) as index of mitophagic process in HAVICs from 15 ARA and 22 CAVS treated or not with rapamycin. Scale bar: 5 μm. Each value is the mean of 20 cells (4 technical and 5 biological replicates). (*D*) Immunoblot detection of cell death in HAVICs lysates. TUBB was used as loading marker; cleaved PARP, RIP, and CAS3 as apoptotic and necrotic markers. This is representative of three biological replicates. (*E*) Quantification of Annexin V fluorescent signal as apoptotic marker in HAVICs from 15 ARA and 22 CAVS treated or not with rapamycin. Each value is the mean of 10 observations (2 technical and 5 biological replicates). (*F*) Quantification of PI fluorescent signal as necrotic marker in HAVICs from 15 ARA and 22 CAVS treated or not with rapamycin. Each value is the mean of 10 observations (2 technical and 5 biological replicates). (*G*) Quantification of extracted alizarin red on HAVICs from 15 ARA and 22 CAVS patients untreated and treated for 7 days with rapamycin; representative images are shown. Each value is the mean of 10 observations (2 technical and 5 biological replicates). (*H*) Cytosolic basal Ca^{2+} concentration and cytosolic Ca^{2+} response upon agonist-induced in on HAVICs from 15 ARA and 22 CAVS patients untreated and treated with rapamycin, quantified using FURA-2AM. Each value is the mean of 20 cells (4 technical and 5 biological replicates). FCCP, carbonyl cyanide-4-(trifluoromethoxy)phenylhydrazone; Rot-AA, rotenone and antimycin A; MRC, maximal respiration capacity. *P*-values have been obtained by performing one-way ANOVA test for multiple comparisons and *t*-test for comparisons between two groups. *P-value <0.05; **P-value <0.01; ***P-value <0.001.

occur during aortic calcification. Future studies will be dedicated to deep investigate about this possibility.

In conclusion, we demonstrated that autophagy and mitophagy pathways are active and increased in CAVS. We also show for the first time multiple that aortic calcification provokes important mitochondrial alterations, including an aged mitochondrial population, suppressed biogenesis, Ca^{2+} dysregulation, and low ATP formation. Such alterations could be in part responsible for cell death and for the osteogenic-driven calcification process and suggest that, although autophagy and mitophagy are expressed at high level, the activation of these catabolic processes is not sufficient to counteract the dangerous phenotype. Accordingly, by potentiating them with rapamycin, at least *in vitro*, reduces cell death and partially restore Ca^{2+} dysregulation.

4.1 Perspectives

From this study, general mitophagy manifests as a crucial 'biomarker', apparently more sensitive than autophagy in the calcification process of the valve. The fact that in some correlations between CAVS and the severity of disease or the calcification grade, the statistical significance has not been reached, could be due to the reason that the population was in principle selected as mostly homogeneous as possible to answer to Aim 1. For this reason, further studies should be undertaken with larger population size and by adjusting inclusion/exclusion criteria to address these secondary endpoints. Moreover, also rapamycin treatment should be further investigated by translating this study in animal models and by using a combination of anti-inflammatory and pro-autophagic drugs.

4.2 Limitations

Although the interesting results, we believe this study shows few limitations that we mention as follows.

The first limitation derives from the use of the control population (ARA). We know that different molecular pathways and shear stress may be active in this type of disease compared to CAVS, but being our study focused on the study of autophagy and mitophagy on severely calcified valve samples and that our ethical committee approved these patients (ARA) as single source of control, we had no choice to find other strategies in the study design.

The second limitation refers to the effective role of autophagy and mitophagy in CAVS. We clearly demonstrate that autophagy and mitophagy are sustained in CAVS and, when boosted, they ameliorate the pathological status. Despite this, our findings are not sufficient to exclude that these catabolic processes may be also a possible cause of the disease.

The last one is focused on the correlation analysis between serum biomarkers and the calcification grade of the valves. Being our CAVS population mostly homogeneous, it does not present itself as the ideal condition to perform and achieve these correlations.

Supplementary material

Supplementary material is available at *Cardiovascular Research* online.

Authors' contributions

G.M. conceived the project, performed experiments, and wrote the manuscript; S.P. performed experiments and wrote the manuscript; G.P. performed experiments; P.C., E.M., S.C., and A.A. enrolled patients, provided and analysed all clinical data; C.G. and P.P. supervised and corrected the biological part of the final manuscript; G.C. and R.F. supervised and corrected the clinical part of the final manuscript.

Conflict of interest: The authors declare no conflict of interest.

Data availability

The data underlying this article are available in the article and in its Supplementary material online.

References

1. Nkomo VT, Gardin JM, Skelton TN, Gottdiener JS, Scott CG, Enriquez-Sarano M. Burden of valvular heart diseases: a population-based study. *Lancet* 2006;**368**: 1005–1011.
2. Garcia-Rodriguez C, Parra-Izquierdo I, Castanos-Mollor I, Lopez J, S, Roman JA, S, Crespo, M. Toll-like receptors, inflammation, and calcific aortic valve disease. *Front Physiol* 2018;**9**:201.
3. Cho KI, Sakuma I, Sohn IS, Jo SH, Koh KK. Inflammatory and metabolic mechanisms underlying the calcific aortic valve disease. *Atherosclerosis* 2018;**277**:60–65.
4. Farrar EJ, Huntley GD, Butcher J. Endothelial-derived oxidative stress drives myofibroblastic activation and calcification of the aortic valve. *PLoS One* 2015;**10**:e0123257.
5. Pedriali G, Morciano G, Patergnani S, Cimaglia P, Morelli C, Mikus E, Ferrari R, Gasbarro V, Giorgi C, Wieckowski MR, Pinton P. Aortic valve stenosis and mitochondrial dysfunctions: clinical and molecular perspectives. *Int J Mol Sci* 2020;**21**:4899.
6. Rajamannan NM, Subramaniam M, Rickard D, Stock SR, Donovan J, Springett M, Orszulak T, Fullerton DA, Tajik AJ, Bonow RO, Spelsberg T. Human aortic valve calcification is associated with an osteoblast phenotype. *Circulation* 2003;**107**: 2181–2184.
7. Galluzzi L, Vitale I, Aaronson SA, Abrams JM, Adam D, Agostinis P, Alnemri ES, Altucci L, Amelio I, Andrews DW, Annicchiarico-Petruzzelli M, Antonov AV, Arama E, Baehrecke EH, Barlev NA, Bazan NG, Bernassola F, Bertrand MJM, Bianchi K, Blagosklonny MV, Blomgren K, Borner C, Boya P, Brenner C, Campanella M, Candi E, Carmona-Gutierrez D, Cecconi F, Chan FK, Chandel NS, Cheng EH, Chipuk JE, Cidlowski JA, Ciechanover A, Cohen GM, Conrad M, Cubillos-Ruiz JR, Czabotar PE, D'Angiolella V, Dawson TM, Dawson VL, De Laurenzi V, De Maria R, Debatin KM, DeBerardinis RJ, Deshmukh M, Di Daniele N, Di Virgilio F, Dixit VM, Dixon SJ, Duckett CS, Dynlacht BD, El-Deiry WS, Elrod JW, Fimia GM, Fulda S, Garcia-Saez AJ, Garg AD, Garrido C, Gavathiotis E, Golstein P, Gottlieb E, Green DR, Greene LA, Gronemeyer H, Gross A, Hajnoczky G, Hardwick JM, Harris IS, Hengartner MO, Hetz C, Ichijo H, Jaattela M, Joseph B, Jost PJ, Juin PP, Kaiser WJ, Karin M, Kaufmann T, Kepp O, Kimchi A, Kitsis RN, Klionsky DJ, Knight RA, Kumar S, Lee SW, Lemasters JJ, Levine B, Linkermann A, Lipton SA, Lockshin RA, Lopez-Otin C, Lowe SW, Luedde T, Lugli E, MacFarlane M, Madeo F, Malewicz M, Malorni W, Manic G, Marine JC, Martin SJ, Martinou JC, Medema JP, Mehlen P, Meier P, Melino S, Miao EA, Molkentin JD, Moll UM, Munoz-Pinedo C, Nagata S, Nunez G, Oberst A, Oren M, Overholtzer M, Pagano M, Panaretakis T, Pasparakis M, Penninger JM, Pereira DM, Pervaiz S, Peter ME, Piacentini M, Pinton P, Prehn JHM, Puthalakath H, Rabinovich GA, Rehm M, Rizzuto R, Rodrigues CMP, Rubinsztein DC, Rudel T, Ryan KM, Sayan E, Scorrano L, Shao F, Shi Y, Silke J, Simon HU, Sistigu A, Stockwell BR, Strasser A, Szabadkai G, Tait SWG, Tang D, Tavernarakis N, Thorburn A, Tsujimoto Y, Turk B, Vanden Berghe T, Vandenabeele P, Vander Heiden MG, Villunger A, Virgin HW, Vousden KH, Vucic D, Wagner EF, Walczak H, Wallach D, Wang Y, Wells JA, Wood W, Yuan J, Zakeri Z, Zhivotovsky B, Zitvogel L, Melino G, Kroemer G.

Molecular mechanisms of cell death: recommendations of the Nomenclature Committee on Cell Death 2018. *Cell Death Differ* 2018;**25**:486–541.

8. Zhang H, Bosch-Marce M, Shimoda LA, Tan YS, Baek JH, Wesley JB, Gonzalez FJ, Semenza GL. Mitochondrial autophagy is an HIF-1-dependent adaptive metabolic response to hypoxia. *J Biol Chem* 2008;**283**:10892–10903.

9. Shirakabe A, Zhai P, Ikeda Y, Saito T, Maejima Y, Hsu CP, Nomura M, Egashira K, Levine B, Sadoshima J. Drp1-dependent mitochondrial autophagy plays a protective role against pressure overload-induced mitochondrial dysfunction and heart failure. *Circulation* 2016;**133**:1249–1263.

10. Jahania SM, Sengstock D, Vaitkevicius P, Andres A, Ito BR, Gottlieb RA, Mentzer RM Jr. Activation of the homeostatic intracellular repair response during cardiac surgery. *J Am Coll Surg* 2013;**216**:719–726.

11. Morciano G, Patergnani S, Bonora M, Pedriali G, Tarocco A, Bouhamida E, Marchi S, Ancora G, Anania G, Wieckowski MR, Giorgi C, Pinton P. Mitophagy in cardiovascular diseases. *J Clin Med* 2020;**9**:892.

12. Kaludercic N, Maiuri MC, Kaushik S, Fernandez AF, de Bruijn J, Castoldi F, Chen Y, Ito J, Mukai R, Murakawa T, Nah J, Pietrocola F, Saito T, Sebti S, Semenzato M, Tsansizi L, Sciarretta S, Madrigal-Matute J. Comprehensive autophagy evaluation in cardiac disease models. *Cardiovasc Res* 2020;**116**:483–504.

13. Somers P, Knaapen M, Kockx M, van Cauwelaert P, Bortier H, Mistiaen W. Histological evaluation of autophagic cell death in calcified aortic valve stenosis. *J Heart Valve Dis* 2006;**15**:43–47.

14. Deng XS, Meng X, Venardos N, Song R, Yamanaka K, Fullerton D, Jaggers J. Autophagy negatively regulates pro-osteogenic activity in human aortic valve interstitial cells. *J Surg Res* 2017;**218**:285–291.

15. Carracedo M, Persson O, Saliba-Gustafsson P, Artiach G, Ehrenborg E, Eriksson P, Franco-Cereceda A, Back M. Upregulated autophagy in calcific aortic valve stenosis confers protection of valvular interstitial cells. *Int J Mol Sci* 2019;**20**:1486.

16. Castellazzi M, Patergnani S, Donadio M, Giorgi C, Bonora M, Bosi C, Brombo G, Pugliatti M, Seripa D, Zuliani G, Pinton P. Autophagy and mitophagy biomarkers are reduced in sera of patients with Alzheimer's disease and mild cognitive impairment. *Sci Rep* 2019;**9**:20009.

17. Meng X, Ao L, Song Y, Babu A, Yang X, Wang M, Weyant MJ, Dinarello CA, Cleveland JC Jr, Fullerton DA. Expression of functional Toll-like receptors 2 and 4 in human aortic valve interstitial cells: potential roles in aortic valve inflammation and stenosis. *Am J Physiol Cell Physiol* 2008;**294**:C29–C35.

18. Carelli V, Musumeci O, Caporali L, Zanna C, La Morgia C, Del Dotto V, Porcelli AM, Rugolo M, Valentino ML, Iommarini L, Maresca A, Barboni P, Carbonelli M, Trombetta C, Valente EM, Patergnani S, Giorgi C, Pinton P, Rizzo G, Tonon C, Lodi R, Avoni P, Liguori R, Baruzzi A, Toscano A, Zeviani M. Syndromic parkinsonism and dementia associated with OPA1 missense mutations. *Ann Neurol* 2015;**78**:21–38.

19. Patergnani S, Giorgi C, Maniero S, Missiroli S, Maniscalco P, Bononi I, Martini F, Cavallesco G, Tognon M, Pinton P. The endoplasmic reticulum mitochondrial calcium cross talk is downregulated in malignant pleural mesothelioma cells and plays a critical role in apoptosis inhibition. *Oncotarget* 2015;**6**:23427–23444.

20. Hernandez G, Thornton C, Stotland A, Lui D, Sin J, Ramil J, Magee N, Andres A, Quarato G, Carreira RS, Sayen MR, Wolkowicz R, Gottlieb RA. MitoTimer: a novel tool for monitoring mitochondrial turnover. *Autophagy* 2013;**9**:1852–1861.

21. Bonora M, Wieckowski MR, Sinclair DA, Kroemer G, Pinton P, Galluzzi L. Targeting mitochondria for cardiovascular disorders: therapeutic potential and obstacles. *Nat Rev Cardiol* 2019;**16**:33–55.

22. Giorgi C, Marchi S, Pinton P. The machineries, regulation and cellular functions of mitochondrial calcium. *Nat Rev Mol Cell Biol* 2018;**19**:713–730.

23. Saito T, Nah J, Oka SI, Mukai R, Monden Y, Maejima Y, Ikeda Y, Sciarretta S, Liu T, Li H, Baljinnyam E, Fraidenraich D, Fritzky L, Zhai P, Ichinose S, Isobe M, Hsu CP, Kundu M, Sadoshima J. An alternative mitophagy pathway mediated by Rab9 protects the heart against ischemia. *J Clin Invest* 2019;**129**:802–819.

24. Noda T, Ohsumi Y. Tor, a phosphatidylinositol kinase homologue, controls autophagy in yeast. *J Biol Chem* 1998;**273**:3963–3966.

25. Castellazzi M, Patergnani S, Donadio M, Giorgi C, Bonora M, Fainardi E, Casetta I, Granieri E, Pugliatti M, Pinton P. Correlation between auto/mitophagic processes and magnetic resonance imaging activity in multiple sclerosis patients. *J Neuroinflammation* 2019;**16**:131.

26. Patergnani S, Castellazzi M, Bonora M, Marchi S, Casetta I, Pugliatti M, Giorgi C, Granieri E, Pinton P. Autophagy and mitophagy elements are increased in body fluids of multiple sclerosis-affected individuals. *J Neurol Neurosurg Psychiatry* 2018;**89**:439–441.

27. Vives-Bauza C, Zhou C, Huang Y, Cui M, de Vries RL, Kim J, May J, Tocilescu MA, Liu W, Ko HS, Magrane J, Moore DJ, Dawson VL, Grailhe R, Dawson TM, Li C, Tieu K, Przedborski S. PINK1-dependent recruitment of Parkin to mitochondria in mitophagy. *Proc Natl Acad Sci USA* 2010;**107**:378–383.

28. Nah J, Miyamoto S, Sadoshima J. Mitophagy as a protective mechanism against myocardial stress. *Compr Physiol* 2017;**7**:1407–1424.

29. Civiletto G, Dogan SA, Cerutti R, Fagiolari G, Moggio M, Lamperti C, Beninca C, Viscomi C, Zeviani M. Rapamycin rescues mitochondrial myopathy via coordinated activation of autophagy and lysosomal biogenesis. *EMBO Mol Med* 2018;**10**:e8799.

30. Deepa SS, Walsh ME, Hamilton RT, Pulliam D, Shi Y, Hill S, Li Y, Van Remmen H. Rapamycin modulates markers of mitochondrial biogenesis and fatty acid oxidation in the adipose tissue of db/db mice. *J Biochem Pharmacol Res* 2013;**1**:114–123.

31. Villa-Cuesta E, Holmbeck MA, Rand DM. Rapamycin increases mitochondrial efficiency by mtDNA-dependent reprogramming of mitochondrial metabolism in Drosophila. *J Cell Sci* 2014;**127**:2282–2290.

Translational perspective

The findings from this study provide evidence for new molecular targets involving mitochondrial quality control mechanisms becoming dysregulated in CAVS. These pathways should be considered as amenable for a combination of new therapies in humans for three reasons: (i) no pharmacological treatments are still available to slow down the development of advanced CAVS, (ii) being calcification a recurring pathway, and (iii) the targets proposed are druggable by existing drugs used in the clinic for different purposes. This work also suggests a serum biomarker to be highly related to the stage of disease and the calcification grade of the valve.